

COMPARISON OF FATIGUE RESISTANCE OF DOG-BONE AND HOURGLASS-SHAPED HARDOX 450 STEEL SPECIMENS

Denisa STRAKOVÁ*, František NOVÝ, Lukáš ŠIKYŇA, Miroslav NESLUŠAN

Faculty of Mechanical Engineering, University of Žilina, Žilina, Slovak Republic

*corresponding author, denisa.strakova@uniza.sk

This study compares the fatigue resistance of two standardized specimen geometries – dog-bone and hourglass-shaped – made from Hardox 450 high-strength steel. Rotating bending fatigue tests evaluated differences in fatigue durability. Strain gauge measurements and the FEM analysis showed hourglass specimens had more uniform stress distribution and lower concentration effects. Fatigue tests revealed an 8% higher fatigue limit for the hourglass specimens, probably due to the lack of localized stress concentration at the transition between the radius and the cylindrical section. These findings contribute to understanding how standardized specimen geometries influence fatigue performance.

Keywords: fatigue testing; geometry; Hardox 450.



Articles in JTAM are published under Creative Commons Attribution 4.0 International.
Unported License <https://creativecommons.org/licenses/by/4.0/deed.en>.
By submitting an article for publication, the authors consent to the grant of the said license.

1. Introduction

High-strength steels play a critical role in industries such as construction, automotive, and aerospace, where their ability to withstand cyclic loading is essential for ensuring the long-term reliability and safety of structural components. Fatigue resistance, a key material property, directly impacts the performance and durability of components subjected to repeated loading. Among the many factors influencing fatigue performance, the geometry of the specimen plays a significant role in stress distribution and in the way cracks initiate and propagate during loading cycles. Understanding how different geometries affect fatigue behaviour is therefore crucial for optimizing the design and reliability of components (Chaurasiya *et al.*, 2023; Okuda *et al.*, 2019).

The shape and size of fatigue test specimens, such as dog-bone and hourglass geometries, can lead to variations in stress concentrations and gradients under cyclic loading. These differences can significantly influence the material's fatigue life and its susceptibility to crack propagation, which are of key importance to an engineering design. Fatigue testing provides valuable data on how materials perform under these conditions, but reliable testing methods are necessary to capture a comprehensive understanding of fatigue behaviour across a range of stress levels (Pan *et al.*, 2024; Hultgren & Barsoum, 2020).

This study aims to explore how the geometry of high-strength steel fatigue test specimens influences their ability to endure cyclic loading. By investigating the effects of specimen shape on stress distribution and fatigue life, this research aims to provide information to help design



Ministry of Science and Higher Education
Republic of Poland

The publication has been funded by the Polish Ministry of Science and Higher Education under the Excellent Science II programme "Support for scientific conferences".

The content of this article was presented during the 40th Danubia-Adria Symposium on Advances in Experimental Mechanics, Gdańsk, Poland, September 24–27, 2024.

more durable and efficient components. Accurate fatigue data is essential for guiding the material selection and component design, ensuring that structural elements perform optimally in demanding applications (McClung, 1994; Hehenberger & Nilsson, 1982).

2. Experimental material and methods

This study investigates the impact of specimen geometry on the fatigue resistance of Hardox 450 high-strength structural steel, whose chemical composition and mechanical properties are given in Table 1.

Table 1. Chemical composition and mechanical properties of Hardox 450 high-strength steel.

C [wt.%]	Si [wt.%]	Mn [wt.%]	Cr [wt.%]	Mo [wt.%]	Nb [wt.%]	B [wt.%]	E [GPa]	$R_{p0.2}$ [MPa]	R_m [MPa]	A [%]	KV_{-40} [J]	HB
0.2	0.39	0.8	0.45	0.01	0.05	0.001	210	1200	1400	10	40	420–475

The samples were fabricated from a 20 mm thick steel sheet via machining. The gauge sections were ground to a surface roughness of $R_a = 0.05 \mu\text{m}$, followed by polishing to achieve a mirror-like finish, ensuring optimal surface quality for subsequent analysis. The surface stresses of hourglass-shaped and dog-bone-shaped test bars (Fig. 1) were analysed using a strain gauge (HBM 1-LY11-1.5/120). Critical radius tolerances were maintained within $\pm 0.02 \text{ mm}$ to ensure accurate stress distribution. The strain gauge was positioned at the central part of the gauge length on the opposite side of the applied bending moment. The test bars were subjected to a gradually increasing bending moment, starting from an initial value of $M_o = 2451.7 \text{ Nmm}$ and progressing incrementally up to a maximum of 26968.2 Nmm . The strain gauge detected the strain change, and the stress on the test bars' surface was calculated using DASYLab software. ANSYS Workbench software was used to create the finite element method (FEM) model of the test bars, set the boundary conditions, and carry out the meshing process. Rotating bending fatigue tests were conducted using a Rotoflex machine on two types of test bars: dog-bone and hourglass-shaped. The tests were performed at a loading frequency of $f = 30 \text{ Hz}$.

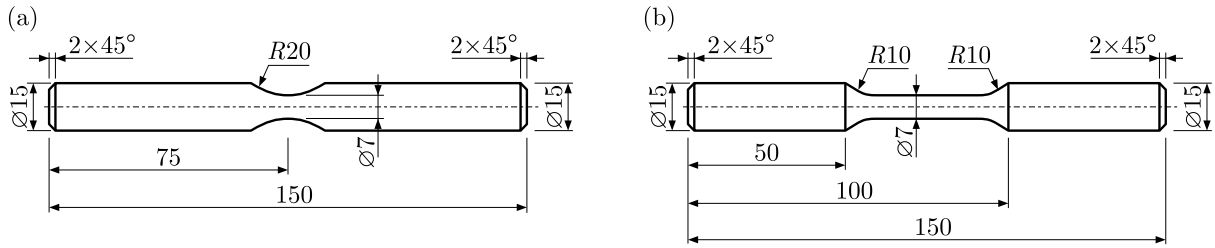


Fig. 1. Fatigue test bars with different geometry: (a) hourglass test bar; (b) dog-bone test bar.

3. Results

The FEM analysis identified the maximum stress concentration (σ_{\max}) of 76.3 MPa in the central area of the hourglass-shaped fatigue test bar under a bending load (M_o) of 2451.7 Nmm. The nominal stress at this bending moment was calculated to be 72.8 MPa allowing to calculate the stress concentration at the critical location, $K_t = 1.05$. In the FEM simulation of a dog-bone-shaped fatigue test bar under the same bending load (Fig. 2), the maximum stress of $\sigma_{\max} = 76.9 \text{ MPa}$ was found in the transition radius area. The stress concentration at this point is a little higher, $K_t = 1.06$.

Figure 3 compares stress changes in the gauge length of fatigue test bars. The stress changes were obtained by the strain gauge measurement (shown in blue) and by FEM analysis (shown

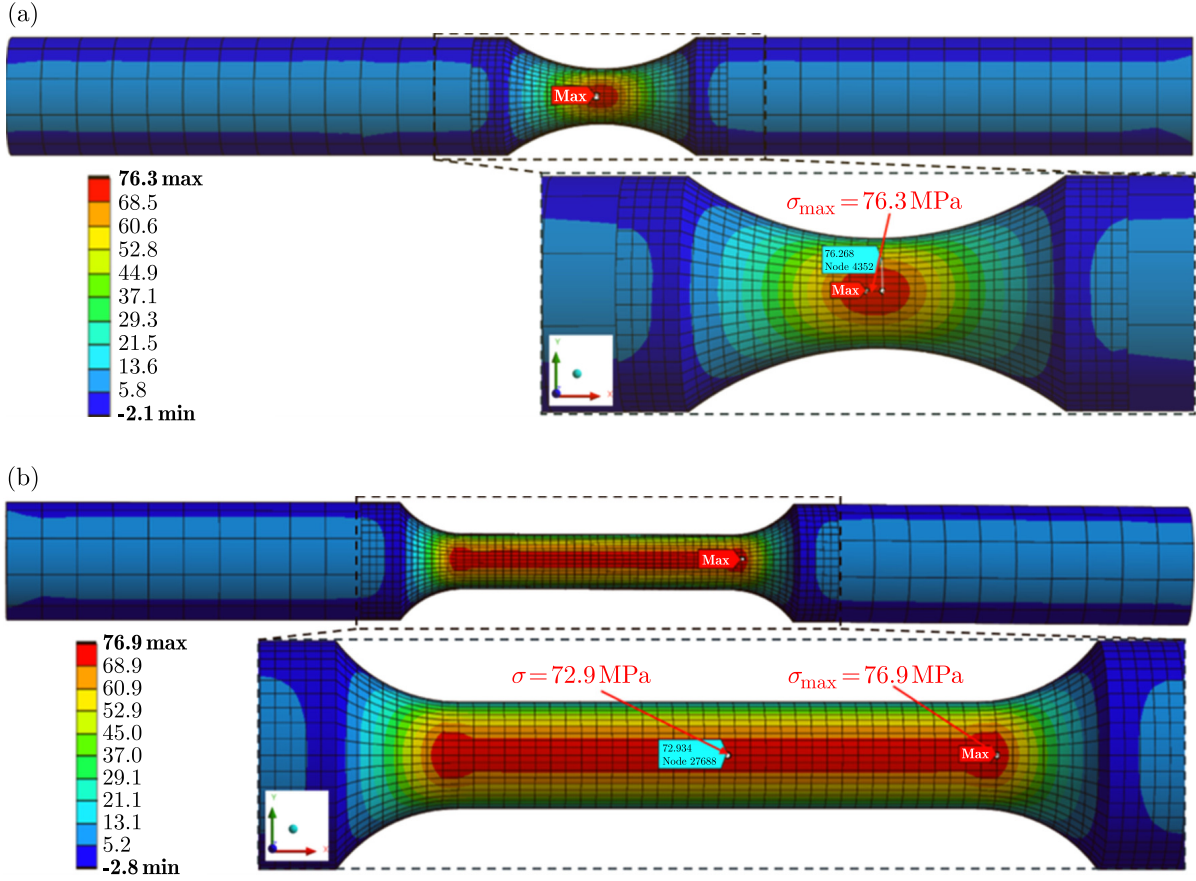


Fig. 2. Stress distribution and maximum concentration on the surface of fatigue test bars with different geometry.

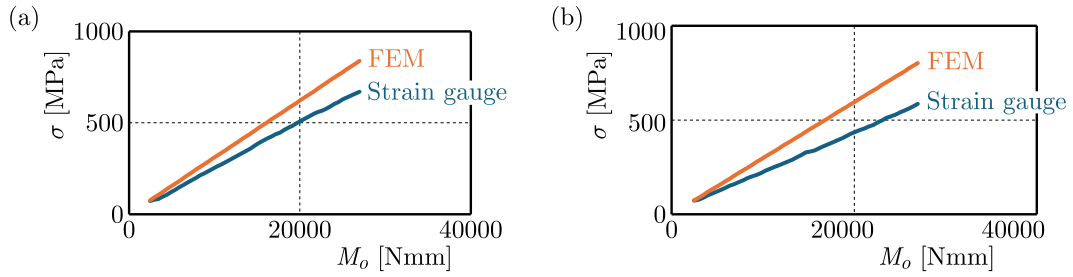


Fig. 3. Stress changes on the surface of the test bars (FEM – orange; strain gauge – blue): (a) hourglass fatigue test bar; (b) dog-bone fatigue test bar.

in orange). The results indicate that at the maximum bending load ($M_{o\max}$) of 26968.3 Nmm for the hourglass-shaped test bar, there was a 25 % difference. For the dog-bone test bar, there was a 37 % difference under the same bending load. The observed differences are probably caused by errors in the positioning of the strain gauge. Part of the error may result from the strain gauge being adhered at an angle, while another part may arise from the test specimen being slightly rotated during the measurement. This rotation could lead to a portion of the strain gauge's measuring base not being aligned with the lowest point of the presumed extreme fibre.

Based on the Wöhler curves depicted in Fig. 4, it is evident that the fatigue limit (denoted as σ_c) occurs at a specified number of cycles $N_f = 10^7$. For the hourglass-shaped fatigue test bar, the value of $\sigma_{c1} = 723$ MPa, and for the dog-bone-shaped test bar, the value of $\sigma_{c2} = 670$ MPa.

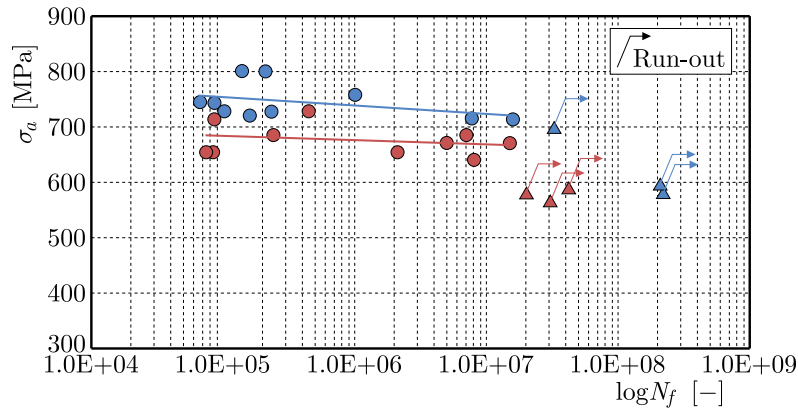


Fig. 4. Wöhler curves: blue – hourglass-shaped fatigue test bar;
red – dog-bone-shaped fatigue test bar.

Hourglass fatigue test bars clearly showed a higher fatigue strength compared to dog-bone test bars. Compared to the study (Ulewicz *et al.*, 2017), which used the same experimental material, but under different testing conditions, the differences between results are likely attributed to differences in specimen geometry, surface preparation, and the specific test conditions, including loading frequency and cooling methods. These factors could influence the material's fatigue behaviour, thereby affecting the fatigue limits observed under different experimental setups.

Fatigue tests showed an 8% higher fatigue limit for hourglass-shaped specimens compared to dog-bone-shaped specimens, primarily due to reduced stress concentration at the radius transition. Finite element analysis confirmed that fatigue failure occurred in the areas of maximum stress concentration: the central shaft for hourglass specimens and the transition radius for dog-bone specimens (Fig. 5). This highlights the significant role of specimen geometry in fatigue performance.

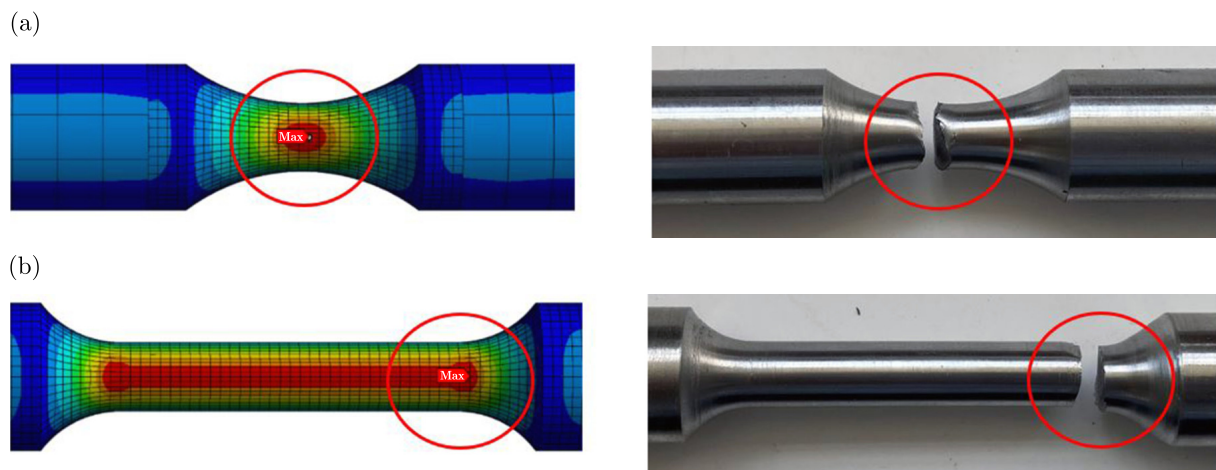


Fig. 5. Regions of maximum stress concentration and fatigue failure in test bars with different geometry:
(a) hourglass test bar; (b) dog-bone test bar.

Fractographic analysis in Fig. 6 revealed subsurface fatigue crack initiation in hourglass-shaped specimens, while surface initiation was observed in dog-bone specimens. Both specimen types showed transcrystalline fatigue failure with striations and ductile fracture with fine dimple morphology in the final fracture zone.

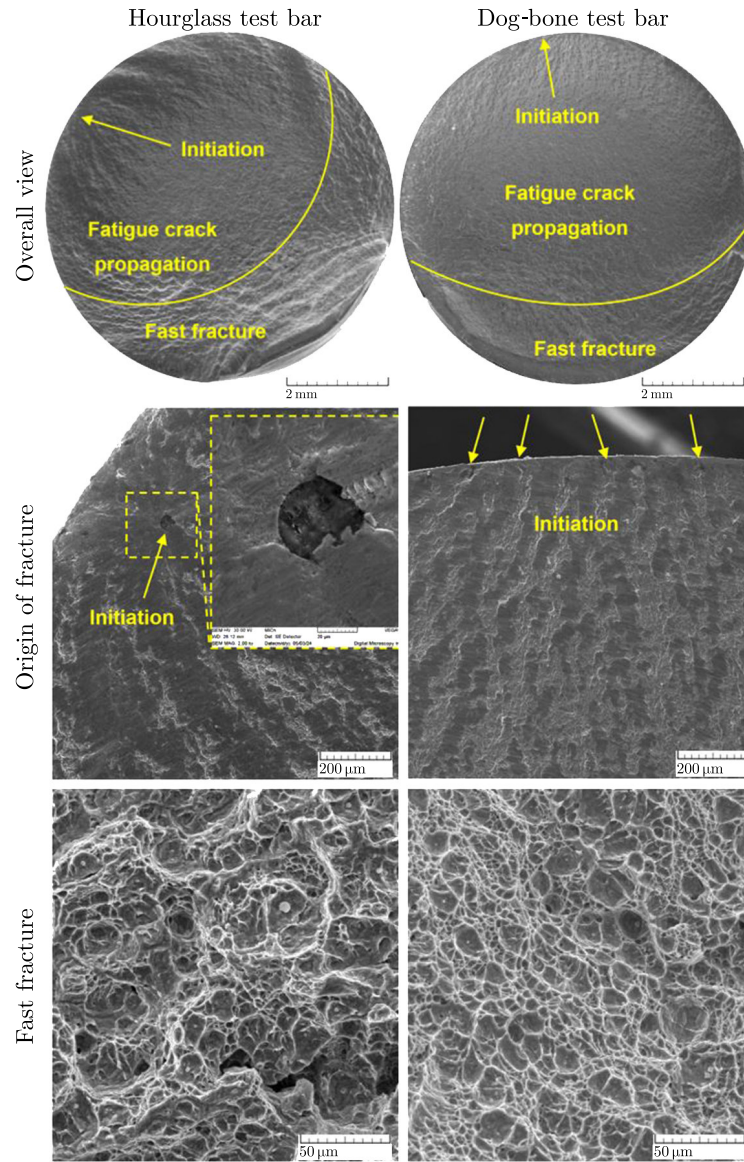


Fig. 6. Fractographic analysis of fractured surfaces after fatigue testing of test bars with different geometry.

4. Conclusions

This study highlights the influence of specimen geometry on the fatigue resistance of Hardox 450 high-strength structural steel. Based on the findings, the following conclusions can be drawn:

- experimental and computational evaluations revealed significant differences in stress concentration patterns between the two geometries. The hourglass test bar exhibited a more uniform and favourable stress distribution compared to the dog-bone counterpart, suggesting its superior design for reducing stress concentrations;
- the hourglass specimens exhibited an 8 % higher fatigue limit than the dog-bone specimens, primarily due to reduced local stress concentration at the radius transition. This highlights the significant impact of specimen geometry on fatigue performance;
- distinct crack initiation modes were observed: subsurface initiation in hourglass specimens and surface initiation in dog-bone specimens. Both exhibited transgranular fatigue failure with characteristic fine dimple fracture morphology, underlining consistent failure mechanisms across geometries.

While the standardized corner radii of both test specimens represent typical structural geometries, small variations could influence fatigue performance. A larger radius may reduce stress concentration and improve fatigue resistance, but the impact depends on other factors such as specimen size, loading conditions, and surface quality.

Acknowledgments

The Slovak Ministry of Education, Science, Research, and Sport's Scientific Grant Agency funded the research under contract VEGA no. 1/0741/21 and the Slovak Research and Development Agency under contract no. APVV-20-0427.

References

1. Chaurasiya, R., Maji, P., & Mukhopadhyay, G. (2023). High cycle fatigue behaviour of advanced high strength steel sheet (HS1000) in automotive application. *Materials Today: Proceedings* (in press). <https://doi.org/10.1016/j.matpr.2023.09.120>
2. Hehenberger, M., & Nilsson, J.O. (1982). A stress analysis of bending fatigue specimens using the finite element method. *International Compressor Engineering Conference*. Paper 381. <https://docs.lib.purdue.edu/icec/381>
3. Hultgren, G., & Barsoum, Z. (2020). Fatigue assessment in welded joints based on geometrical variations measured by laser scanning. *Welding in the World*, 64(11), 1825–1831. <https://doi.org/10.1007/s40194-020-00962-8>
4. McClung, R.C. (1994). Finite element analysis of specimen geometry effects on fatigue crack closure. *Fatigue & Fracture of Engineering Materials & Structures*, 17(8), 861–872. <https://doi.org/10.1111/j.1460-2695.1994.tb00816.x>
5. Okuda, K., Ogawa, K., Ichikawa, Y., Shiozaki, T., & Yamaguchi, N. (2019). Influence of microstructure on fatigue property of ultra high-strength steels. *Fracture and Structural Integrity*, 13(48), 125–134. <https://doi.org/10.3221/IGF-ESIS.48.15>
6. Pan, M., Yang, L., Zheng, X., Mao, H., Kong, Y., & Du, Y. (2024). Numerical simulation of fatigue fracture in gradient high-strength steel: effects of carbides and gradient structure on stress-strain response and crack propagation behavior. *Journal of Materials Science*, 59(27), 12757–12780. <https://doi.org/10.1007/s10853-024-09907-8>
7. Ulewicz, R., Szataniak, P., Novy, F., Trsko, L., & Bokuvka, O. (2017). Fatigue characteristics of structural steels in the gigacycle region of loading. *Materials Today: Proceedings*, 4(5), 5979–5984. <https://doi.org/10.1016/j.matpr.2017.06.081>

*Manuscript received December 5, 2024; accepted for publication March 6, 2025;
published online May 29, 2025.*